Pergamon

0038-1101(95)00210-3

Solid-State Electronics Vol. 40, Nos 1-8, pp. 43-46, 1996

0038-1101/96 \$15.00 + 0.00

EFFICIENT GREEN LUMINESCENCE FROM A TYPE-II NEIGHBORING CONFINEMENT STRUCTURE REALIZED IN AN AlP/GaP SYSTEM

F. ISSIKI[1], S. FUKATSU[2], T. OHTA[1] and Y. SHIRAKI[1]

[1]Research Center for Advanced Science and Technology (RCAST), The University of Tokyo, 4-6-1 Komaba, Meguro-ku, Tokyo 153, Japan

[2]Department of Pure and Applied Sciences, The University of Tokyo, 3-8-1 Komaba, Meguro-ku, Tokyo 153, Japan

Abstract—Highly efficient green luminescence was observed from a new class of quantum confined geometry referred to as neighboring confinement structure (NCS). The photoluminescence (PL) intensity of AlP/GaP NCSs was even higher than that of a 300-period AlP/GaP superlattice (SL), and the PL of the NCS exhibited much improved immunity against thermal quenching compared to the SLs. The luminescence origin of the NCS was confirmed from the well width dependence of the PL peak shift, and the main luminescence line was assigned to no-phonon from a phonon-resolved PL study.

1. INTRODUCTION

Advanced growth technologies in recent years have enabled observation of clear luminescence from indirect gap semiconductor structures such as AlGaP and strained SiGe systems [1–5]. In particular, the AlGaP system has attracted vast interest, not only from the scientific viewpoint, but also from the standpoint of technological application for green light emitters. The light emitting efficiency is still the central point of arguments. Fortunately, the small lattice mismatch in this AlGaP system facilitates the fabrication of good AlP/GaP superlattices (SLs) and hence the extensive studies of recent years. The luminescence efficiency of SLs is, however, not high enough for device applications such as lasers, and its luminescence origin has not yet been clarified.

In this study, we present a comparative luminescence study for type-II $Al_xGa_{1-x}P$ quantum confined systems and SLs, and the observation of an unexpectedly high efficiency of luminescence for a new type of $Al_xGa_{1-x}P$ QW structure with type-II band lineup, referred to as *neighboring confinement structure* (NCS), as shown in Fig. 1a. It is shown that the PL intensity of the NCS is higher than that of a 300-period SL.

The band lineup of the $Al_xGa_{1-x}P$/GaP system has been shown to be of type-II (staggered) with indirect band gap, over the entire composition range [6]. Therefore the radiative recombination is essentially of indirect nature both in real-space and k-space. The staggered band lineup has been regarded as the drawback of the $Al_xGa_{1-x}P$/GaP system, since the oscillator strength of the optical transition is significantly reduced due to spatial separation of electrons and holes. For example, in the usual QW as shown in Fig. 1b (AlP QW) and/or Fig. 1c (GaP QW), the electrons and holes are plausibly understood to possess small recombination probability, unlike the type-I system.

The NCS is proposed to overcome such a limitation. This structure confines electrons and holes separately in thin neighboring layers (AlP and GaP) with the outer $Al_xGa_{1-x}P$ ($x \approx 0.5$) cladding layers. The electrons are confined in the AlP layer while the holes are confined in the GaP layer. The outer $Al_xGa_{1-x}P$ layers are essential to establish carrier buildup at the centered heterointerface. Then the penetrated wavefunctions of the electron and hole overlap each other as the thickness of the confining layers (AlP and GaP) is decreased. The increased overlap of the wavefunctions is expected to lead to an increased recombination probability of the electrons and holes and hence enhanced luminescence.

A calculation within the effective mass approximation shows that, for an AlP 15 Å/GaP 15 Å NCS sandwiched between the $Al_xGa_{1-x}P$ of $x = 0.5$, the normalized overlap integral of the envelope wavefunctions exceeds 30%, which is fairly close to that of a type-I QW. This is of sufficient magnitude to compensate for the loss of the otherwise smaller transition probability inherent to the type-II system.

In addition, it is expected that the Γ-X mixing of the wavefunctions induced by the thin AlP layer enhances the recombination probability due to translational symmetry breaking. This effectively relaxes the strict selection rule of the momentum-conserving optical transitions and allows for the dominance of no-phonon transitions. The present scheme can be also applied to such material systems consisting of the type-II band lineup as strained $Si_{1-x}Ge_x$ lattice-matched to SiGe [7–9].

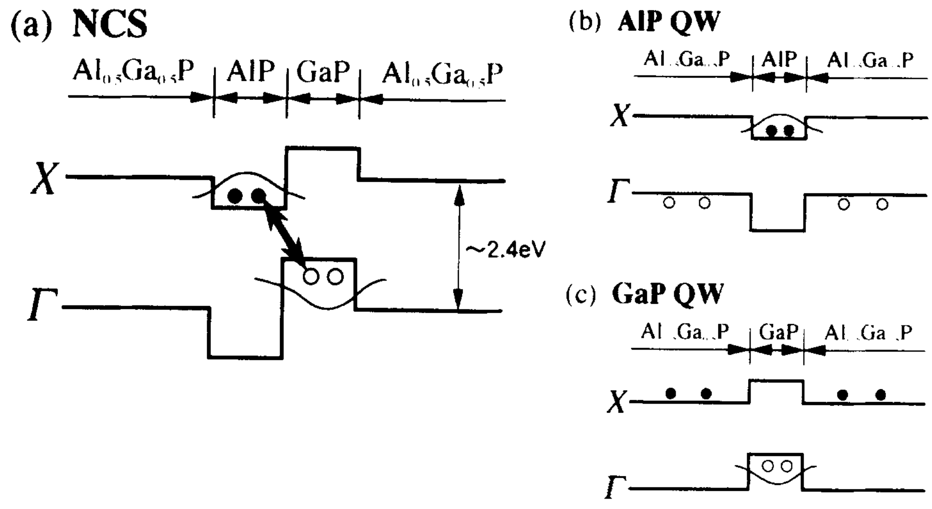

Fig. 1. Schematic band lineups of (a) AlP/GaP neighboring confinement structure (NCS), (b) AlP QW and (c) GaP QW. The NCS confines both electrons and holes with the increased overlap of the envelope wavefunctions penetrated across the centered interface.

2. EXPERIMENTAL

All the samples were grown by gas source molecular beam epitaxy (GSMBE) (VG Semicon V80H) using PH_3 and elemental Ga and Al. The substrates were nominally undoped GaP (100) wafers. The sample structure of AlP 18 Å/GaP 9 Å NCS is shown in the inset of Fig. 2. After the growth of a 3000 Å buffer layer, the barrier layers and active layers were grown at around 620°C which was the lowest temperature that $4x$ patterns in the reflection high energy electron diffraction (RHEED) could be observed during the growth of the GaP buffer layer. This low-temperature growth helps prevent thickness fluctuation of the GaP layer. During the growth of the GaP cap layer, the substrate temperature was ramp raised to 650°C and the whole structure was annealed for 5 min. The composition of the $Al_xGa_{1-x}P$ barrier was confirmed to be within the range of $0.50 < x < 0.54$ from X-ray diffraction spectra. The control SL was a 300-period AlP/GaP SL separately grown at a substrate temperature of 700°C, and its structure was confirmed to be $(AlP)_{3.5}/(GaP)_{3.5}$ (3.5 ML ≈ 9.6 Å) from the satellite peak analysis of X-ray diffraction.

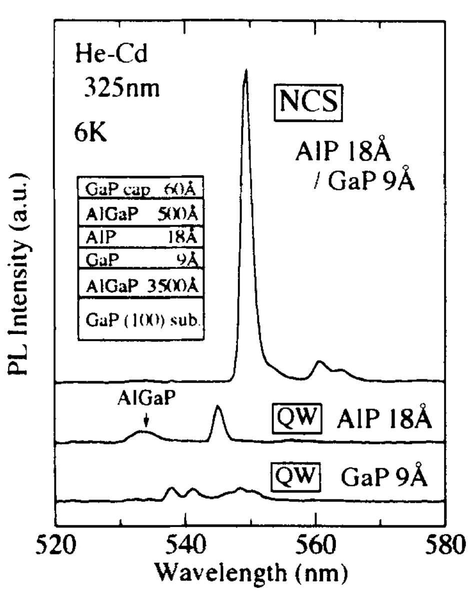

Fig. 2. 6-K PL spectra of NCS and AlP·GaP QWs. The inset shows schematic sample structure of the NCS. The PL intensity of the NCS is much higher than those of QWs, which shows the luminescent enhancement of NCS. The peak shifts are consistent with the quantum confinement as described in Fig. 1.

PL was measured at low temperatures (2–6 K). The exciton source was a cw He-Cd laser (325 nm) and its total power was 20 mW. The laser power density was typically 1.0 W cm^{-2}.

3. RESULTS AND DISCUSSION

Figure 2 compares the PL spectra of the NCS (AlP 18 Å/GaP 9 Å) and AlP QW (18 Å) and GaP QW (9 Å). The PL intensity of the NCS is much higher than those of the AlP and GaP QWs, which shows clear luminescent enhancement of NCS. There are no other pronounced features other than the dominant main peak centered at 549 nm in the PL spectrum of the NCS sample, except for small phonon replicas on the lower energy side. The peak energy difference among samples, AlGaP bulk at 534 nm, GaP QW (the highest peak) at 538 nm, AlP QW at 545 nm, and NCS at 549 nm, is consistent with the band lineup and the associated transition in NCS and QWs as schematically shown in Fig. 1.

Figure 3 shows the temperature dependence of the PL intensity of the NCS (circles) and the SL (triangles). The inset shows 6-K PL spectra of the NCS and the SL. The exciting laser is focused to give a

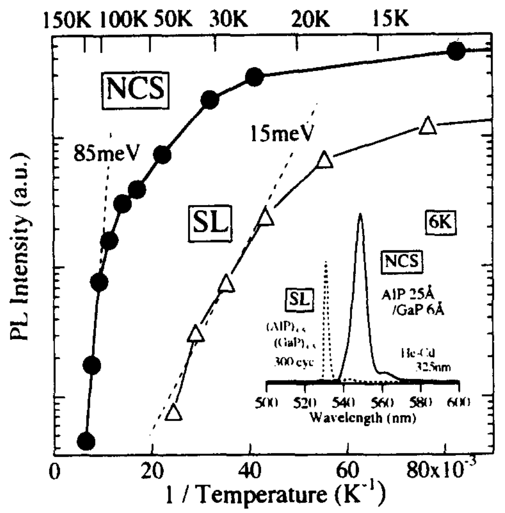

Fig. 3. Temperature dependence of the PL intensity of AlP 25 Å/GaP 6 Å NCS and the control AlP/GaP SL of 300 periods. The inset shows 6-K PL spectra of the NCS (solid line) and the SL (dashed line). Intensity of the NCS sample decreased only $\sim 10^{-1}$ times even at 100 K, while that of the SL sample is completely quenched at 50 K. The activation energies of the thermal roll-off for the NCS and the SL are 85 meV and about 15 meV, respectively.

power density of 25 W cm^{-2}, causing the line broadening and the appearance of a shoulder on the higher energy side. The PL intensity is spectrally integrated including the shoulder, since the shoulder was observed to shift with the main peak, and was also assigned to be luminous from the NCS. The PL intensity of the NCS decreases only by a factor of 10 as the temperature is increased up to 100 K, whereas that of the SL is completely quenched at 50 K. The activation energy of the PL intensity roll-off at higher temperatures for the NCS is 85 meV, which is much improved than that for the SL, approximately 15 meV. Thus, the NCS is seen to offer better immunity against thermal quenching than the SL.

To confirm that the luminescence origin of the NCS is due to the expected spatial indirect transition, we grew two series of multiple NCS (MNCS) samples. In the first set of the samples, the GaP layer thickness was varied from 7 to 22 Å, while the AlP layer thickness was fixed at 20 Å. In the second set, the AlP layer thickness was varied as 13–50 Å, while keeping the GaP layer thickness at 10 Å. It is expected that the MNCS shows quantum-confined peak shift as the thickness of AlP and GaP is varied.

The 6-K PL spectra from the two MNCS samples are shown in Fig. 4. The peaks clearly shift towards the higher energy side with decreasing thickness of the AlP and GaP layers. The maximum confinement shifts of 155 and 99 meV are obtained in the valence band (GaP) and conduction band (AlP), respectively. This is clear evidence that the luminescence of the NCS originates from the optical transition, as sketched in Fig. 1.

A recent study on phonon-resolved PL suggests that the main luminescence line which is dominant in the NCS spectrum is the no-phonon line, which is expected to improve the realization of stimulated emission. Figure 5 shows the shifted PL spectra of the NCS (on logarithmic scale), AlP QW (on logarithmic scale), bulk AlGaP alloy and GaP QWs. Each spectrum was shifted along the horizontal axis so that

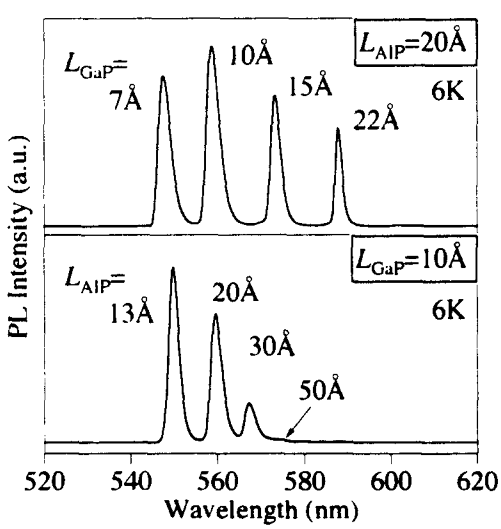

Fig. 4. 6-K PL spectra of the MNCSs. The peaks shift with changing AlP and GaP layer thickness, which reflects the quantum confinement in the conduction and valence band, respectively.

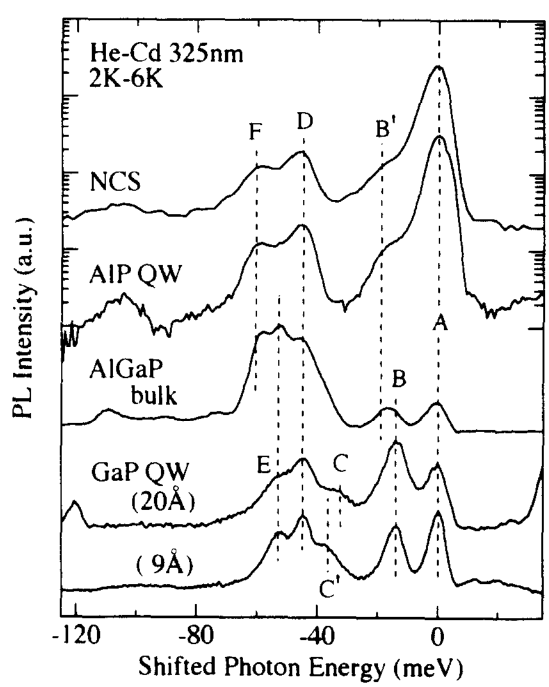

Fig. 5. Shifted PL spectra of the NCS, AlP QW, bulk AlGaP alloy, and GaP QWs. Each spectrum is shifted along the horizontal axis so that the highest energy peak falls on 0 meV (line A). The splitting energies of the peak B ~ F away from the line A well agree with the reported phonon energies.

the highest-energy peak falls on 0 meV (line A). It is clearly seen that the splitting energies of these peaks are fixed, and are not due to quantum size fluctuations or transitions from upper subbands. The energy split of lines B ~ F away from the peak A corresponds well with the reported phonon energies (B(14 meV) with GaP TA(X) of 13 meV, C(32.5 meV) with GaP LA(X) of 31 meV, D(45 meV) with GaP TO(Γ) of 45 meV or LO(X) of 46 meV or TO(X) of 44 meV [10], E(53 meV) with AlP TO(Γ) of 54 meV, and F(60.5 meV) with AlP LO(Γ) of 62 meV [11]). The phonon energies are cited from Ref. [12]. The good agreement indicates that these peak series are phonon-related replicas, and at the same time suggests that the highest-energy peak A is the no-phonon line. The peak B′ can be assigned to AlP TA(X), though its energy is not solicited in the literature. The slight shift between the C and C′ is thought to be due to phonon mode mixing. The more detailed analysis on these assignments will be published separately.

4. CONCLUSION

A new class of AlP/GaP quantum-confined geometry, NCS, was proposed. Efficient green luminescence was observed with considerable immunity against thermal quenching compared to SLs. The well width dependence of the PL of the NCS was investigated, and the luminescent origin of the NCS was confirmed. Phonon-resolved PL study suggests that the main luminescence line of the NCS is due to no-phonon transition.

Acknowledgements—The authors gratefully acknowledge the support and instructions of crystal growth by Y. Seco, and technical supports by S. Otake. This work was in part supported by a Grant-in-Aid from Ministry of Science, Education and Culture. One of the authors (S.F.) gratefully acknowledges the support from Toray Science Foundation, Japan.

REFERENCES

1. A. Morii, H. Okagawa, K. Hara, J. Yoshino and H. Kukimoto, *J. Cryst. Growth* **124**, 772 (1992); A. Morii, I. Ohno, A. Kanda, K. Arai, K. Tokudome, K. Hara, J. Yoshino and H. Kukimoto, *Jap. J. Appl. Phys.* **30**, L1244 (1991); A. Morii, T. Takano, J. Kitamura, K. Hara, H. Kukimoto, J. Yoshino and T. Yasuda, *Solid-State Electron.* **37**, 649 (1994).
2. K. Asami, H. Asahi, T. Watanabe, S. Gonda, H. Okumura and S. Yoshida, *Surf. Sci.* **267**, 450 (1990).
3. A. Sasaki, Xue-Lun Wang and A. Wakahara, *Appl. Phys. Lett.* **64**, 2016 (1994); Xue-Lun Wang, A. Wakahara and A. Sasaki, *Appl. Phys. Lett.* **62**, 888 (1993).
4. U. Menczigar, G. Abstreiter, J. Olajos, H. Grimmeiss, H. Kibbel, H. Presting and E. Kasper, *Phys. Rev.* **B 47**, 4099 (1993).
5. S. Fukatsu, *Solid-State Electron.* **37**, 817 (1994) and references therein.
6. Zh. I. Alferov, D. Z. Garbuzov, S. G. Konnikov, P. S. Kop'ev and V. A. Mishurnyi, *Sov. Phys. Semicond.* **7**, 1449 (1974).
7. R. People, *IEEE J. Quantum Electron.* **22**, 1696 (1986).
8. G. Abstreiter, H. Brugger, T. Wolf, H. Jorke and H. J. Herzog, *Phys. Rev. Lett.* **54**, 2441 (1985).
9. N. Usami, F. Issiki, D. K. Nayak, Y. Shiraki and S. Fukatsu, *Appl. Phys. Lett.* **67**, 524 (1995).
10. B. Pödaar, *Phys. Status Solidi* (b) **120**, 207 (1983).
11. A. Onton, *Proc. of the 10th Int. Conf. on Physics of Semiconductors*, Cambridge/Mass. 1970, USAC, Oak Ridge (1970).
12. Landolt-Börnstein, *Numerical Data and Functional Relationships in Science and Technology* (Edited by O. Madelung) Group III, Vol. 22. Springer, Berlin (1987).